Oxymatrine inhibits TGF-β1-mediated mitochondrial apoptotic signaling in alveolar epithelial cells via activation of PI3K/AKT signaling

TONG FENG[1-3*], RAN DUAN[2,4*], PENGCHENG ZHENG[1], JING QIU[1], QINGYUAN LI[1-3] and WANCHENG LI[1-3]

[1]Department of Respiratory and Critical Care Medicine, The First Affiliated Hospital of Chengdu Medical College, Chengdu, Sichuan 610500; [2]School of Clinical Medicine, Chengdu Medical College; [3]Key Laboratory of Geriatrics Respiratory Disease Education Department of Sichuan, Chengdu, Sichuan 610500; [4]Department of Cardiology, First Affiliated Hospital of Chengdu Medical College, Chengdu, Sichuan 610500, P.R. China

Received August 31, 2022; Accepted January 24, 2023

DOI: 10.3892/etm.2023.11897

Abstract. Although pulmonary fibrosis (PF) causes respiratory failure and death, effective therapies for PF have not been developed. Oxymatrine (OMT), an active ingredient in the Chinese herb *Sophora flavescens*, exerts antifibrotic effects; however, its effect on PF remains unclear. The present study aimed to determine whether OMT decreases transforming growth factor-β1 (TGF-β1)-induced PF in human lung cancer A549 cells by inhibiting apoptosis and targeting the phosphoinositide 3-kinase (PI3K)/protein kinase B (AKT) pathway. To construct a PF cell model, A549 cells were stimulated with TGF-β1. The experimental groups were as follows: control (untreated cells grown in complete medium), TGF-β1 (cells treated with 5 ng/ml TGF-β1), OMT (cells treated with 5 ng/ml TGF-β1 and 0.25, 0.50, or 1.00 mg/ml OMT), and OMT + LY294002 (cells treated with 5 ng/ml TGF-β1, 1.0 mg/ml OMT. and 25 μmol/l LY294002). The effects of OMT on cell morphology (via electron microscopy), apoptosis (via Annexin V-PI staining), mitochondrial apoptosis signaling [using JC-1 method to analyze mitochondrial membrane potential (MMP)], and Bcl-2, as well as Bax expression (via western blotting and reverse transcription-quantitative polymerase chain reaction), were analyzed. OMT significantly protected cells against TGF-β1-induced PF by inhibiting apoptosis. The specific manifestations were cell injury, as evidenced by morphological changes and decreased MMP. Following OMT treatment, the expression of the pro-apoptotic protein Bax increased, whereas that of the anti-apoptotic protein Bcl-2 decreased. The PI3K/AKT-specific inhibitor LY294002 significantly inhibited the ameliorative effects of OMT on TGF-β1-induced apoptosis. Collectively, OMT attenuated TGF-β1-mediated mitochondrial apoptosis of alveolar epithelial cells by activating the PI3K/AKT signaling pathway. Therefore, OMT may be a promising drug for PF treatment.

Introduction

Pulmonary fibrosis (PF) is induced by multiple triggers, including apoptosis of alveolar epithelial cells (AECs), activation of fibroblasts and deposition of large amounts of collagen (1). Although understanding of IPF pathogenesis, diagnostic evaluation and treatment approaches has evolved (2-3), the typical survival time of patients diagnosed with PF is 3-5 years, as highlighted by a previous literature review (4). Currently, pirfenidone and nintedanib are the most common commercially available antifibrotic drugs (5). However, these drugs only slow disease progression and do not restore damaged lung tissue and function (6,7). Additionally, both pirfenidone and nintedanib have strong gastrointestinal adverse effects (6,7). Currently, lung transplantation is the most efficacious therapy for PF (8). However, owing to factors such as the need for donor matching, high cost of surgery, and use of immunosuppressant drugs, the rate of lung transplantation is low, with nearly 4500 performed in 2017, including 32.4% for PF (9). Additionally, compared with patients requiring transplantation for other reasons, patients with PF have a high waiting list mortality rate of 18-67% (8). Therefore, affordable treatments or drugs with low toxicity are needed.

Correspondence to: Professor Wancheng Li, Department of Respiratory and Critical Care Medicine, The First Affiliated Hospital of Chengdu Medical College, 278 Baoguang Avenue, Xindu, Chengdu, Sichuan 610599, P.R. China
E-mail: liwancheng@cmc.edu.cn

*Contributed equally

Abbreviations: AEC, alveolar epithelial cell; AKT, protein kinase B; MMP, mitochondrial membrane potential; OMT, oxymatrine; PBS, phosphate-buffered saline; PF, pulmonary fibrosis; PI3K, phosphoinositide 3-kinase; RT-qPCR, reverse transcription-quantitative polymerase chain reaction; TCM, traditional Chinese medicine; TEM, transmission electron microscope; TGF-β1, transforming growth factor-β1

Key words: pulmonary fibrosis, oxymatrine, apoptosis, PI3K pathway, epithelial cell

The imbalance between fibrogenic and antifibrogenic molecules in the lung may induce apoptosis and prevent normal re-epithelialization of AECs, as well as promote fibroblastic proliferation and alveolar epithelial-mesenchymal transition, all of which are involved in the development of PF (10,11). Ultrastructural studies have revealed that AEC death is notable in the initial phase of PF (12,13). The pulmonary histopathology of patients with PF and bleomycin-induced PF animal models have revealed fibroblastic proliferation in the area of apoptosis of AECs (14,15). Apoptosis of AECs has also been observed in near-normal lung areas (16,17).

During apoptosis, apoptotic signals [such as transforming growth factor β (TGF-β)] induce intracellular cytokine changes, leading to a loss of cellular structural integrity and degradation of DNA and phagocytic clearance. Apoptosis is generally classified into two pathways based on the signaling pathway involved: Endogenous (mitochondrial-mediated) and exogenous (death receptor-mediated) pathways (16). Mitochondria are the control center of cell activity; they provide energy via oxidative phosphorylation and mediate endogenous apoptotic signaling pathways (18). The alteration of mitochondrial transmembrane potential and membrane permeability promotes the activation of downstream apoptosis-associated factors (such as Bax and Bcl-2), leading to apoptosis. BH3-interacting domain death agonist, a Bcl-2 family member, induces intrinsic apoptosis of AECs by suppressing Bcl-2 and upregulating Bax/Bak (19).

The phosphoinositide 3-kinase (PI3K)/protein kinase B (AKT) pathway is a signaling pathway composed of intracellular signaling enzymes (20). PI3K, when activated by extracellular signals, upregulates production of the intracellular secondary messenger phosphatidylinositol-3,4,5-trisphosphate (PIP3) via phosphorylation of phosphatidylinositol-bisphosphate. PIP3 binds to specific docking sites in the pleckstrin homology structural domain of AKT1 and induces conformational changes in AKT1 (21). Activated AKT1 proteins translocate to cellular compartments, such as the cytoplasm and nucleus, where they phosphorylate various substrate proteins, thereby regulating cellular functions such as those associated with proliferative metabolism, migration and survival. Activation of PI3K/AKT has been reported in PF tissue (20,22). Activated AKT can directly regulate the expression of Bcl-2 and other downstream factors, thereby affecting cellular apoptosis (23).

Traditional Chinese medicine (TCM) has been utilized in China for >2,000 years and is an important part of clinical practice. Baicalein, quercetin, and safflower yellow pigment, all extracted from Chinese herbs, effectively alleviate symptoms of fibrosis in experimental animal models (24-26). Furthermore, new dosages of antifibrotic drugs used in TCM have been developed in the form of inhalants, which are convenient to use, increase the concentration of drug in the lungs and exhibit a good effect in the treatment of PF (27,28). Therefore, research on the active components of Chinese herbal medicines may contribute to the development of anti-PF drugs.

Oxymatrine (OMT), a monomer alkaloid isolated from *Sophora flavescens*, has a tetracyclic quinoline structure and is considered to be the primary component responsible for the pharmacological effects of *Sophora flavescens*. These pharmacological effects include anti-oxidative stress (29), anti-inflammatory (30), anti-tissue fibrotic (31), and tumor apoptosis-inducing effects (32). OMT is commonly used in tumor radiotherapy regimes; it is used to treat leukopenia caused by chemotherapy and other factors (33,34). In addition, OMT has been confirmed to regulate apoptosis (35,36). Moreover, it regulates the PI3K/AKT signaling pathway in colitis and hypoxic-ischemic brain damage (37,38). Additionally, OMT significantly alleviates bleomycin-induced PF by inhibiting the expression of inducible nitric oxide synthase (39). However, to the best of our knowledge, the mechanisms of action and role of OMT in the regulation of PF remain unclear.

TGF-β is a key factor that regulates fibrosis and tumorigenesis. TGF-β is a pleiotropic cytokine that has three isoforms: TGF-β1, TGF-β2 and TGF-β3. These isoforms regulate biological processes, including embryogenesis, cell differentiation, organ development and immune response (40). TGF-β1 is involved in PF as a strong pro-fibrotic mediator that promotes epithelial-mesenchymal transition, apoptosis of epithelial cells, migration, production of other pro-fibrotic mediators, recruitment of circulating fibroblasts and activation, and proliferation and transformation of fibroblasts into myofibroblasts (41). TGF-β1 was the first cellular factor found to induce interstitial-epithelial transformation in the alveolar epithelium (41). TGF-β1-induced A549 cell line is an established model of PF (42). Therefore, the present study aimed to determine whether OMT decreases TGF-β1-induced PF by inhibiting apoptosis and whether this mechanism is associated with the PI3K/AKT pathway.

Materials and methods

Materials. The human lung AEC line A549 was purchased from Beijing Solarbio Science & Technology Co., Ltd. Cellular short tandem repeat typing of DNA from the A549 cell line showed no human cell crossover contamination and the DNA matched the DNA of the A549 strain found in the cell bank by 100%.

TGF-β1 was purchased from Sizhe Technology (cat. no. CHE0029, http://www.sagene.com.cn/ms/). OMT was purchased from Macklin (cat. no. 16837-52-8). LY294002 was purchased from MedChemExpress (cat. no. 154447-36-6). JC-1 Mitochondrial Membrane Potential (MMP) Assay kit was purchased from Beyotime Institute of Biotechnology (cat. no. C2006). Annexin V-FITC/PI Fluorescence Double Staining Apoptosis Detection kit was purchased from Elabscience Biotechnology, Inc. (cat. no. E-CK-A211). Antibodies against β-actin (rabbit; cat. no. AF7018), Bcl-2 (mouse; cat. no. BF9103) and phosphorylated (p)-PI3K (rabbit; cat. no. AF3241) were obtained from Affinity Biosciences, Ltd. Antibodies against AKT (rabbit; cat. no. YT0185) and p-AKT (rabbit; cat. no. YP0006) were purchased from Ruiying Biotechnology. Antibody against PI3K (mouse; cat. no. Bsm33219m) was purchased from Bioss, Inc.; that against BAX (rabbit; cat. no. GB11690) was purchased from Wuhan Seville Biotechnology Co., Ltd. The 5X All-In-One MasterMix (with AccuRT Genomic DNA Removal kit) and EvaGreen Express 2X qPCR MasterMix-No Dye were purchased from Applied Biological Materials, Inc. (cat. no. G492; MasterMix-ES).

The automatic medical PCR analysis system was from Shanghai Hongshi Medical Technology Co., Ltd.

(cat. no. SLAN-96S). The electrophoresis apparatus (PowerPac Basic) was purchased from Bio-Rad Laboratories, Inc. The chemiluminescence imaging system (ChemiScope 6100), image acquisition software (ChemiScope Capture) and analysis software (ChemiScope analysis) were purchased from Shanghai Qingxiang Science Instrument Co., Ltd. The flow cytometer (CytoFLEX) was purchased from Beckman Coulter, Inc. YOUPU series ultrapure water heater was procured from Sichuan YOUPU Ultrapure Technology Co., Ltd. (cat. no. upr-ii-10t). A low-speed centrifuge was purchased from Scilogex, LLC (cat. no. dm0412s). A transmission electron microscope (TEM) was purchased from Hitachi, Ltd. (cat. no. HT7700).

Cell culture and treatment. A549 cells were cultured in RPMI-1640 medium (Solebro; cat. no. 31800) supplemented with 10% fetal bovine serum (Merck KGaA; cat. no. F8687) in a 5% CO_2 incubator at 37˚C. The medium was changed once daily, digested and passaged using 0.25% trypsin (Merck KGaA; cat. no. 9002). The cells were passaged at 80% confluency. Cells of the same passage were used in each experiment and the experiments were repeated using different batches of cells. A cell model of PF was induced using 5 ng/ml TGF-β1, as previously described (34). The experimental groups were as follows: Control (cells were cultured in complete medium without any treatment); TGF-β1 (cells were treated with 5 ng/ml TGF-β1); OMT (cells were treated with 5 ng/ml TGF-β1 and 0.25, 0.50 or 1.00 mg/ml OMT); and OMT + LY294002 (cells were treated with 5 ng/ml TGF-β1, 1 mg/ml OMT, and 25 μmol/l LY294002). The OMT + LY294002 group was pretreated with LY294002 for 2 h, and then TGF-β1 and OMT were administered simultaneously. OMT 0.25, 0.5, and 1.0 mg/ml concentrations were selected based on a previous study in which OMT attenuated fibroblast proliferation (43). All treatments were performed for 48 h at 26˚C.

Cell resuspension. The cryopreserved cells (stored in liquid nitrogen/-80˚C freezer) were placed in a water bath (37˚C) for ~1 min to allow liquid from cells to thaw. Subsequently, 1 ml cell suspension was pipetted into a 15-ml centrifuge tube on an ultraclean stage and 10 ml complete medium [50 ml fetal bovine serum into 500 ml RPMI 1640 medium (including 1% penicillin/streptomycin antibody)] was added. After centrifugation at 200 x g for 6 min in an ordinary centrifuge at room temperature (~26˚C), the supernatant was discarded and 2 ml complete medium was added to the cell pellet, which was suspended in the medium using a pipette to mix. The cell suspension was seeded on a 10-cm cell culture dish at a 1:3 ratio of inoculation. Thereafter, the cells were mixed in the dish and incubated at 37˚C under 5% CO_2 for culture.

Cell passages. Cell passaging was performed when the cells reached ~90% confluence. The complete medium, pancreatin and sterile 1X phosphate-buffered saline (PBS) were pre-warmed to 37˚C. The old culture medium was discarded, and the cells in the dish were washed twice with PBS, after which 1 ml 0.25% pancreatin EDTA (0.01%) digestion solution was added to cover the bottom of the dish. The digestion was performed at 26˚C until the bottom of the dish showed a frosted appearance. The dish was placed under an inverted light microscope to observe whether the intercellular space had increased and whether the cells had shrunk and were free-floating at the bottom of the dish, indicating that digestion was complete. The digestion was terminated by addition of complete medium (3 ml), and cells were suspended by pipetting gently against the bottom of the dish. On an ultraclean table, the suspension was pipetted into a 15-ml centrifuge tube and centrifuged at 26˚C at 200 x g for 6 min. The supernatant was discarded, complete medium was added, and the cell pellet was resuspended using a pipette. Subsequently, cells were seeded on a 10-cm cell culture dish at a 1:3 ratio, followed by mixing the cells in the dish and incubation at 37˚C under 5% CO_2 for culture.

Cell cryopreservation. The cells at the top of the culture were collected, and cell freezing was performed when the cells reached ~90% confluence. The digested cells were centrifuged to pellet the cells at 200 x g for 5 min. The supernatant was discarded, and 1 ml pre-chilled cell cryoprotectant solution (formulated by adding 1 ml dimethyl sulfoxide to 9 ml fetal bovine serum; the serum was configured as a mixture and stored at -20˚C after mixing) was added to the cell pellet. Cells were resuspended using a pipette and aliquoted into cryovials. Following gradient freezing (4˚C for 30 min, -20˚C for 1 h and -80˚C for 24 h), the cryopreserved cells were transferred to a liquid nitrogen tank for storage at 26˚C.

Morphological changes. The cells were digested with trypsin for ~1 min at 26˚C. Subsequently, an inverted light microscope was used to check whether the cells were round and bright and whether the intercellular gap had increased, after which, 500 μl complete medium was added immediately to stop digestion. The cell suspension was transferred to a 15-ml bullet head centrifuge tube and centrifuged at 1,000 x g for 5 min at 25˚C. After discarding supernatant, 200 μl 2.5% glutaraldehyde was added and the cells were fixed overnight at 4˚C. Subsequently, the cells were washed three times with PBS, fixed with 1% osmium for 2 h at 26˚C and washed three times with PBS. The cells were subjected to ethanol and acetone gradient ascending dehydration at 26˚C (50% ethanol and dehydrated for 10 min → 70% ethanol for 10 min → 90% ethanol for 10 min → 90% acetone for 10 min → 100% acetone three times for 10 min each), epoxy resin infiltration, and embedding for 2 h. Samples (50-70-nm thick) were obtained using ultramicrotome sectioning; the sections were subjected to double staining with uranyl acetate and lead citrate (cells were stained with 2% uranyl acetate for 20 min and lead dye solution for 5 min at 26˚C and observed and imaged under a TEM at x1,500 magnification).

MMP analysis. Cells ($1x10^6$) were centrifuged at 300 x g for 5 min at 26˚C. The supernatant was discarded and cells were resuspended in 500 μl JC-1 working solution and incubated for 20 min at 37˚C. Following centrifugation (300 x g, 5 min) at 26˚C , the cells were washed once with pre-cooled 1X JC-1 assay buffer. Subsequently, cells were centrifuged (300 x g, 5 min) at 26˚C and supernatant was discarded. The cells were resuspended in 500 μl 1X JC-1 assay buffer. Flow cytometry (CytoFLEX, Beckman Coulter, Inc.) using JC-1 MMP Assay kit was used to analyze MMP. The data were analyzed using

CytExpert 2.3 (Beckman Coulter, Inc.). A 488-nm laser was selected, and the FITC and phycoerythrin (PE) channels were used.

Cell apoptosis assay. Following aforementioned drug treatment, the cells were digested with 0.25% trypsin (without EDTA) for 6 min at 26˚C and collected. The cells were washed twice with pre-cooled PBS and resuspended in 100 μl 1X binding buffer. Annexin V-FITC (5 μl) was added and the cells were incubated at 2-8˚C for 15 min in the dark. Subsequently, 10 μl PI was added and cells were incubated at 2-8˚C under dark conditions for 5 min. Thereafter, apoptosis was analyzed using flow cytometry.

Western blotting. RIPA lysis solution (Beyotime Institute of Biotechnology; cat. no. P0013B) was used to extract total protein from A549 cells. The total protein concentration was determined using the bicinchoninic acid method and bovine serum albumin (PA115, Tiangen Biochemical Technology Co., Ltd.) as a standard. Proteins (1 ml) were separated using SDS-PAGE on a 10% gel. After transferring proteins onto PVDF membranes, 5% skimmed milk powder in 5% PBS-Tween was used to block the membranes for 1 h at 26˚C. Primary antibodies against Bcl-2, BAX, PI3K, p-PI3K, AKT, p-AKT and β-actin (all 1:1,000) were added, and the membranes were incubated overnight at 4˚C. The corresponding secondary antibody (1:3,000, Wuhan Saiwei Biotechnology Co., Ltd., GB23303 GB23301) was added, and the membranes were incubated at 26˚C for 2 h. Subsequently, a Pro-light horseradish peroxidase chemiluminescence substrate (Merck KGaA; cat no. WBKLS) was added and signals of the immunoreactive protein bands were captured on a film (ChemiScope analysis 1.0, Shanghai Qingxiang Science Instrument Co., Ltd.), which was developed in a dark room. The expression of the protein of interest was normalized to the expression of β-actin, an internal reference protein.

Reverse transcription-quantitative (RT-q)PCR. A549 cell suspension ($2x10^5$ cells/ml) was treated with RNase and subjected to total cellular RNA extraction using TRIzol® reagent (Invitrogen; Thermo Fisher Scientific, Inc.), according to the manufacturer's instructions. Total RNA concentration was quantified using a nucleic acid analyzer (Kaiao Technology Co., Ltd.; cat. no. k2900). RT was performed to obtain cDNA, which was used for PCR amplification using the primer pairs listed in Table I. For qPCR, a 20 μl reaction mixture containing 2 μl cDNA, 1.2 μl 7.5 μM primer mix of forward and reverse primers, 10 μl 2X qPCR master mix, and 6.8 μl double-distilled water was used. The thermocycling conditions were as follows: Initial denaturation at 95˚C for 10 min, followed by 40 cycles of denaturation at 95˚C for 10 sec and annealing and extension at 60˚C for 30 sec. The amplification and dissolution curves were obtained, and the data were analyzed using the $2^{-\Delta\Delta Cq}$ method (44). β-actin was used as the housekeeping gene.

Statistical analysis. The experimental data were analyzed using GraphPad Prism 9 (GraphPad Software, Inc.). Data that followed a normal distribution are expressed as the

Table I. Primer pairs for reverse transcription-quantitative PCR.

Gene	NCBI gene ID	NCBI search no.	Forward primer, 5'→3'	Reverse primer, 5'→3'	Product length, bp	Melting temperature, ˚C
β-actin	60	NM_001101	AATCTGGCACCACACCTTCTACAA	GGATAGCACAGCCTGGATAGCAA	172	60
PI3K	5290	NM_006218	CGGTGACTGTGTGGGACTTATTGAG	TGTAGTGTGTGGCTGTTGAACTGC	111	60
AKT	207	NM_001014431	TCCTCCTCAAGAATGATGGCA	GTGCGTTCGATGACAGTGGT	181	60
Bax	581	NM_001291428	CGAACTGGACAGTAACATGGAG	CAGTTTGCTGGCAAAGTAGAAA	157	60
Bcl-2	596	NM_000633	GACTTCGCCGAGATGTCCAG	GAACTCAAAGAAGGCCACAATC	129	60
Caspase-3	836	NM_001354777	CCAAAGATCATACATGGAAGCG	CTGAATGTTTCCCTGAGGTTTG	185	60

NCBI, National Center for Biotechnology Information.

mean ± standard deviation (n=3). One-way ANOVA followed by Tukey's post hoc test was used for comparison between ≥3 groups. P<0.05 was considered to indicate a statistically significant difference.

Results

OMT attenuates TGF-β1-induced morphology damage. The ultrastructure of cells in each group was observed under a TEM (Fig. 1). In the control group, A549 cells showed clear nucleoli in small clumps with uniform nucleoplasm and cytoplasm without swelling, no discernible swelling of the mitochondria, homogeneous matrix, orderly cristae and no discernible dilatation of the rough endoplasmic reticulum (Fig. 1A). Additionally, the structure of each organelle was clear. In the TGF-β1 group, A549 cells showed loss of structural integrity, nuclear pyknosis, increased cytoplasmic electron density, blebbing, unclear organelle structure and vacuolated intra-organelle autophagosomes (Fig. 1B). In the 0.25 mg/ml OMT group, nuclear pyknotic electron density was increased, chromatin was homogenized, cytoplasmic electron density was increased, and a notable number of vacuoles in organelles and small number of autophagosomes were present in A549 cells (Fig. 1C). Additionally, pyknosis of mitochondria was observed. In the 0.5 mg/ml OMT group, A549 cells exhibited indented nuclear membranes and relatively uniform nucleoplasm. Additionally, the cytoplasm was uniform without discernible swelling and few vacuoles in organelles and autophagosomes in cytoplasm were observed (Fig. 1D). Notable mitochondrial pyknosis was observed. In the 1.0 mg/ml OMT group, A549 cells exhibited indented nuclear membranes and a relatively uniform nucleoplasm and cytoplasm without discernible swelling. A small number of vacuoles in organelles and a few lipid droplets were present in the cells. Furthermore, the structure of the mitochondria and endoplasmic reticulum was unremarkable (Fig. 1E). The images of the cell culture are shown in Fig. S1.

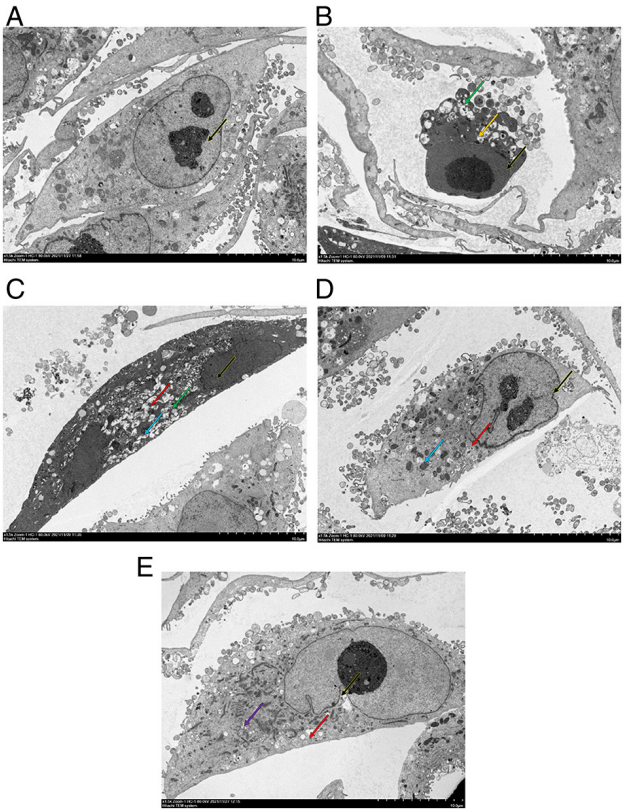

Figure 1. OMT inhibits TGF-β1-induced ultrastructural changes in A549 cells. (A) Control (black arrow, clear nucleoli). (B) TGF-β1 (black arrow, nuclear pyknosis; green arrow, autophagosomes; yellow arrow, cell membrane blebbing). (C) 0.2 (black arrow, nuclear pyknosis; green arrow, autophagosomes; blue arrows, mitochondrial pyknosis; and red arrow, organelle vacuole), (D) 0.5 (black arrow, nuclear pyknosis; blue arrow, mitochondrial pyknosis; and red arrow, organelle vacuolization), and (E) 1.0 mg/ml (Black arrows, pyknosis; purple arrows, lipid droplets; red arrows, organelle vacuole) OMT. Magnification, x1,500. OMT, oxymatrine.

OMT prevents TGF-β1-induced apoptosis of A549 cells. Annexin V-FITC/PI assay indicated that the percentage of apoptotic cells considerably increased following TGF-β1 treatment; however, following OMT treatment, the fraction of apoptotic cells decreased considerably. This suggested that OMT treatment can reduce the TGF-β1-induced apoptosis of A549 cells (Figs. 2 and S2).

OMT attenuates TGF-β1-induced dissipation of MMP. TGF-β1-treated A549 cells showed strong intracellular green fluorescence and weak red fluorescence, indicating that the MMP decreased following TGF-β1-induced damage of AECs. Following OMT treatment, cells showed increased red and decreased green fluorescence, suggesting that OMT alleviated abnormal MMP induced by TGF-β1 (Fig. 3, Fig. S3).

OMT inhibits cell apoptosis by activating mitochondrial apoptotic signaling. The expression of apoptosis-associated proteins downstream of the PI3K pathway was investigated (Fig. 4). The expression of Bax (pro-apoptotic protein) was upregulated following TGF-β1 treatment compared with that in the control group; however, treatment with OMT inhibited upregulation of Bax expression. Conversely, expression of Bcl-2 was inhibited by TGF-β1 treatment but increased by OMT treatment. These results suggested that OMT inhibited TGF-β1-mediated activation of mitochondrial apoptotic signaling. In the OMT + LY294002 group, expression of Bax was notably inhibited and that of Bcl-2 was enhanced compared with those in the OMT group (Fig. 5A). PCR analysis indicated that OMT could enhance mRNA expression of Bcl-2 and inhibit Bax compared with the control group (Fig. 5B). These findings suggested that OMT inhibited TGF-β1-mediated activation of mitochondrial apoptotic signaling.

OMT inhibits cell apoptosis by activating PI3K pathway. The expression of proteins associated with the PI3K/AKT signaling pathway was examined (Fig. 5). The total protein expression of PI3K and AKT in the experimental groups was not significantly different. TGF-β1-treated cells showed upregulation of p-AKT and p-PI3K expression compared with the control group. Additional OMT treatment augmented these effects. Moreover, upregulation of p-AKT and p-PI3K was reversed following OMT + LY294002 treatment (Fig. 5A). Collectively, these results suggest that OMT activated the PI3K/AKT pathway.

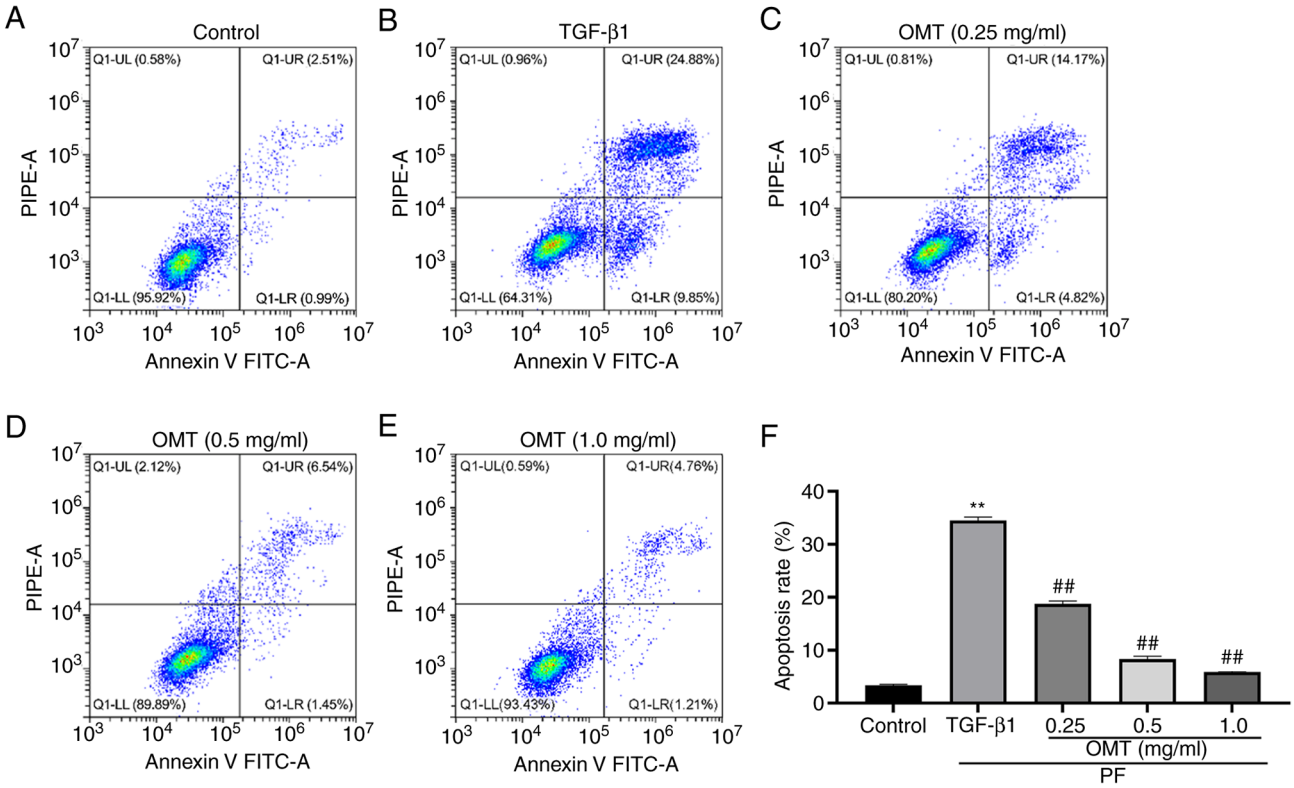

Figure 2. OMT decreases TGF-β1-induced apoptosis of A549 cells. Number of apoptotic A549 cells in (A) control, (B) TGF-β1 and (C) 0.2, (D) 0.5 and (E) 1.0 mg/ml OMT groups. (F) Cell apoptosis rate. **P<0.01 vs. Control; $^{\#\#}$P<0.01 vs. TGF-β1. n=3. Q1-LL, Annexin-V negative and PI-negative (live cells); Q1-LR, Annexin V-positive and PI-negative (early apoptosis); Q1-UR, Annexin V-positive, PI-positive cells (late apoptosis); Q1-UL, Annexin V-negative and PI-positive (necrotic cells); OMT, oxymatrine; PF, pulmonary fibrosis; PIPE-A, phycoerythrin channel detecting PI.

Discussion

Although lung transplantation and medicines (pirfenidone and nintedanib) can be used to treat PF, these therapies are associated with adverse effects. Gastrointestinal and skin-associated adverse events are reported in pirfenidone treatment (45). By contrast, antifibrotic therapy based on natural chemicals may lower the risk of adverse effects while acting on various targets (46). The lipid disorders of lung fibrosis can be corrected upon baicalin treatment. In addition, treatment with dexamethasone does not improve pf but leads to the accumulation of fat in the liver (47). Consequently, the use of natural substances in the treatment of PF is becoming increasingly popular (24-26). The present study investigated if OMT prevents apoptosis in PF and inhibits processes involved in apoptosis.

Apoptosis is a cell death mechanism triggered by activation of certain signals and subsequent gene regulation (48). It is key for clearing cells that have the potential to develop abnormally and preserving homeostasis. The alveolus is the origin of PF and early lesions of PF include alveolar epithelial injury and alveolitis (49). Additionally, apoptosis of AECs is key in the development of PF (50). Studies have demonstrated that OMT exerts its protective effect by inhibiting apoptosis (37,38). Therefore, the present study tested the hypothesis that OMT alleviates PF by inhibiting apoptosis and investigated the potential underlying mechanisms.

AECs are classified into types I and II, of which type I cells are less abundant, accounting for ~15% of alveolar cells. However, the area occupied by type I cells accounts for 95% of the entire alveolar area and their primary function is to maintain alveolar structure and perform gas exchange (51). By contrast, type II cells are abundant, accounting for 85% of alveolar cells, but only 5% of alveolar area. Type II cells proliferate to replace type I cells that are cleared following aging-related cellular damage and essentially function as stem cells; additionally, they synthesize alveolar surfactant, participate in immune regulation, and adjust the fluid balance of the alveolus (52,53). However, type II cells, as alveolar epithelial stem cells, cannot divide sufficiently to replenish damaged type I epithelial cells (11). The injury is repaired by fibroblasts, which proliferate and induce deposition of a large amount of extracellular matrix, leading to PF (54). A549 cells, which are human alveolar basal epithelial cells that exhibit characteristics of type II AECs, are widely used in the study of PF (55,56). These cells were therefore selected for use in the present study to establish a cell model of PF.

A decrease in MMP occurs during apoptosis in all types of cells. Once the MMP decreases, the cell enters the irreversible stage of apoptosis (53). In the present study, MMP of TGF-β1-treated A549 cells increased significantly following OMT treatment. Concurrently, morphological changes and the number of apoptotic cells were also ameliorated by OMT treatment. Bcl-2 family members participate in mitochondria-mediated apoptosis by regulating the release of pro-apoptotic factors via mitochondrial membrane pore formation proteins (57). Bcl-2 localizes to the nuclear and mitochondrial membranes and is widely distributed in hematopoietic and epithelial cells, lymphocytes, and nerve

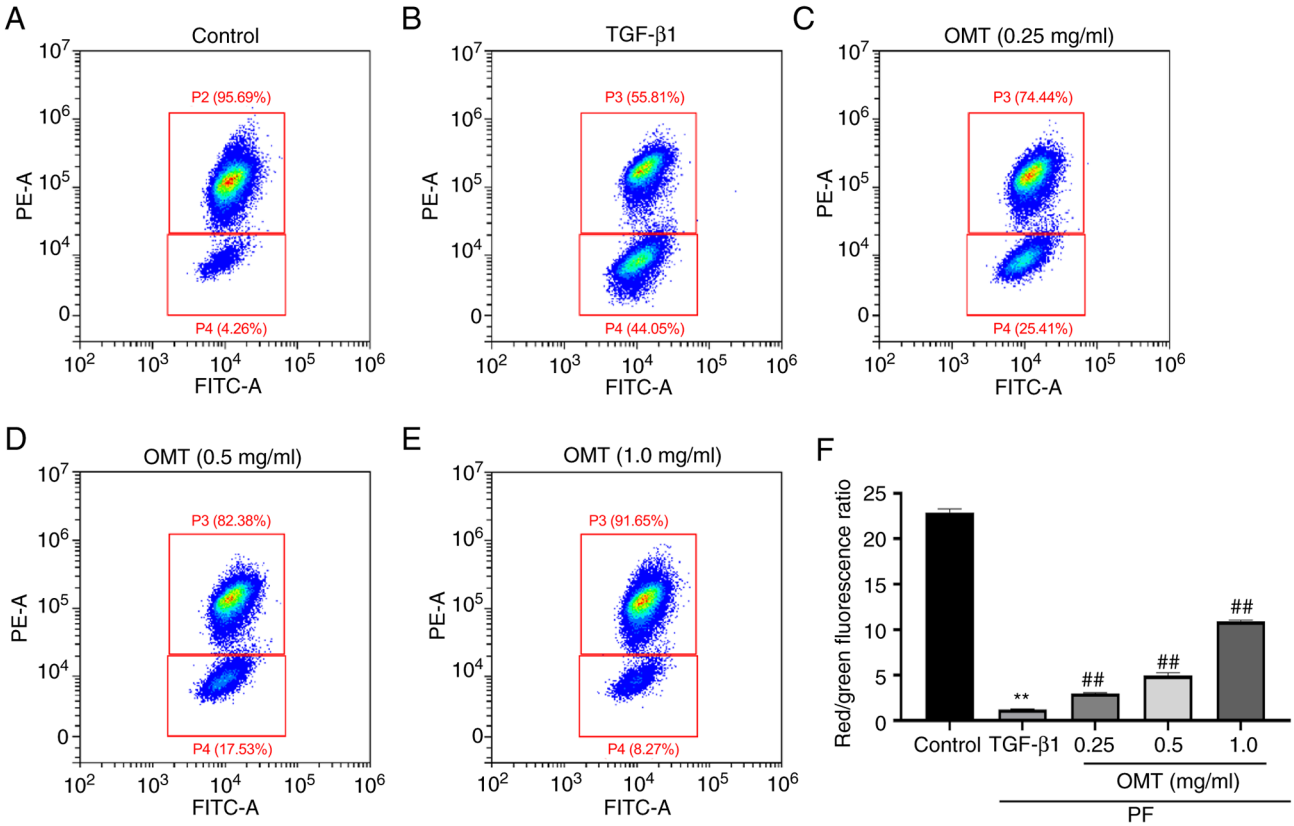

Figure 3. OMT decreases TGF-β1-induced dissipation of MMP in A549 cells. MMP of A549 cells in (A) control, (B) TGF-β1 and (C) 0.2, (D) 0.5 and (E) 1.0 mg/ml OMT groups. (F) Ratio of red to green fluorescence. **P<0.01 vs. control; ##P<0.01 vs. TGF-β1. Experiments were performed in triplicate. OMT, oxymatrine; MMP, mitochondrial membrane potential; PF, pulmonary fibrosis; PE, phycoerythrin.

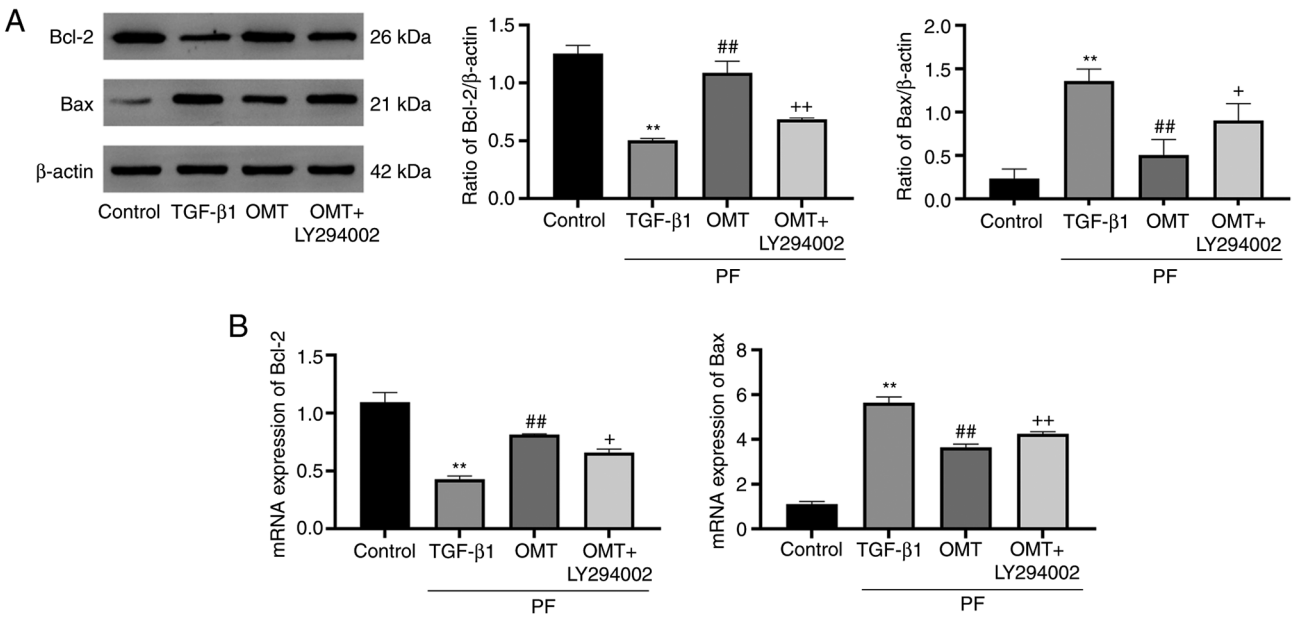

Figure 4. OMT regulates the expression of apoptosis-associated proteins. (A) Western blotting of Bcl-2 and Bax. (B) mRNA levels of Bcl-2 and Bax were determined using reverse transcription-quantitative PCR. **P<0.01 vs. control; ##P<0.01 vs. TGF-β1; +P<0.05 and ++P<0.05 vs. OMT. Experiments were performed in triplicate. OMT, oxymatrine; PF, pulmonary fibrosis.

cells (58). By contrast, pro-apoptotic protein Bax primarily exists in the cytoplasm under normal conditions (59,60). Upon induction of apoptosis, Bcl-2 family proteins are localized to the mitochondrial membrane by various mechanisms, such as isomerization and phosphorylation, causing changes in mitochondrial membrane permeability and initiation of the apoptotic response (18). In the present study, following OMT treatment, expression of the pro-apoptotic gene Bax

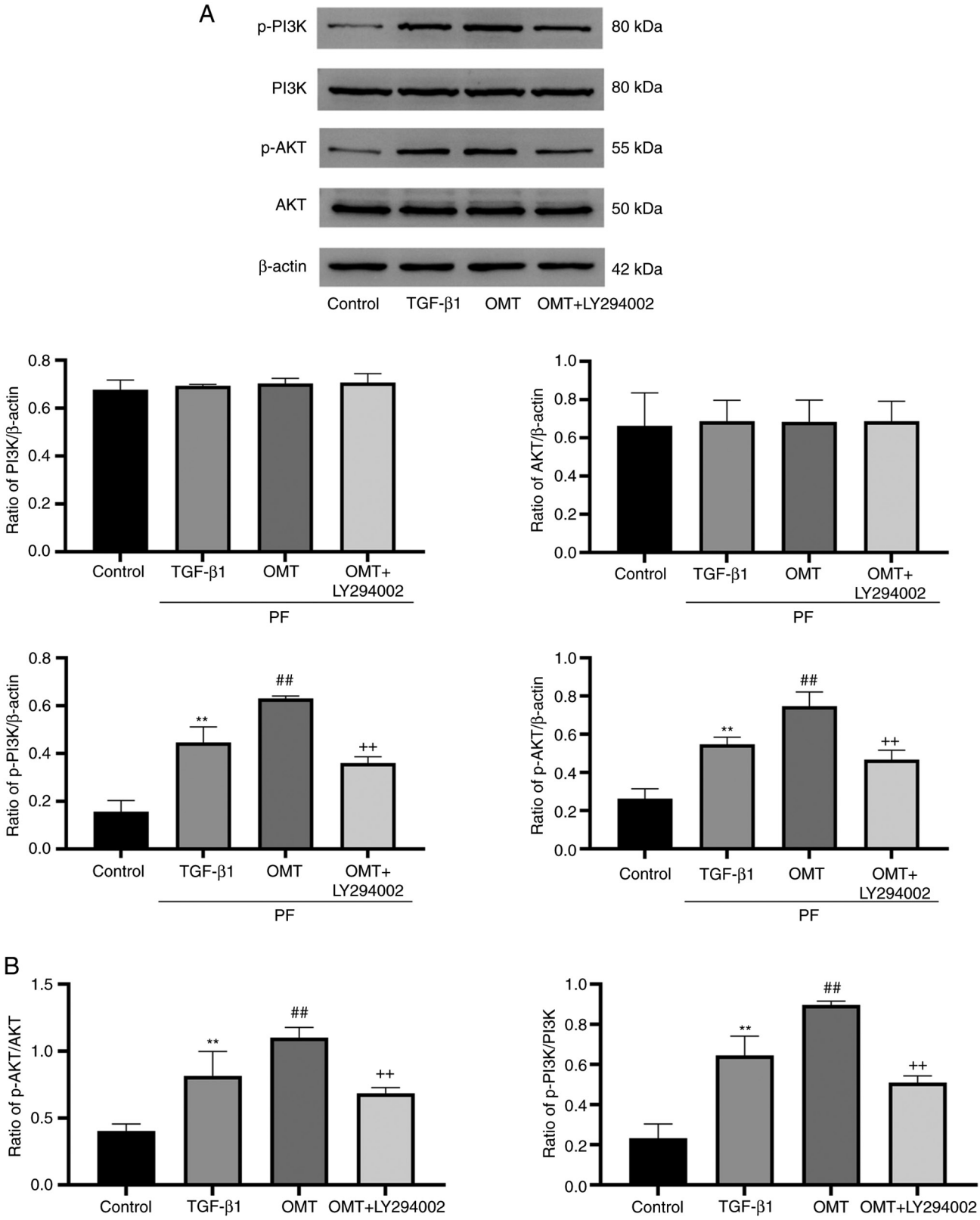

Figure 5. OMT ameliorates TGF-β1-induced pulmonary fibrosis via the PI3K/AKT signaling pathway. (A) Western blotting of PI3K, AKT, p-PI3K and p-AKT. (B) Ratio of p-PI3K/PI3K and p-AKT/AKT. **P<0.01 vs. control; $^{\#\#}$P<0.01 vs. TGF-β1; $^{++}$P<0.05 vs. OMT. Experiments were performed in triplicate. OMT, oxymatrine; PF, pulmonary fibrosis; p, phosphorylated.

significantly decreased, whereas that of the apoptotic-inhibitory gene Bcl-2 significantly increased. These results support the hypothesis that OMT exerts an anti-apoptotic effect through the mitochondrial apoptosis pathway.

The PI3K/AKT pathway is involved in various physiological processes, including apoptosis, proliferation, and metabolism (61). Following phosphorylation, PI3K-activated AKT regulates downstream molecules, including Bad,

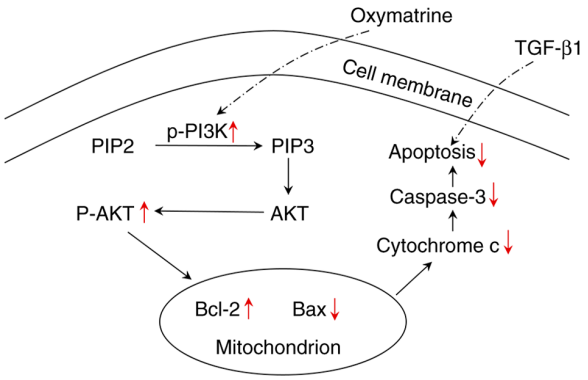

Figure 6. OMT protects against pulmonary fibrosis by inhibiting the apoptosis signaling pathway (red arrow indicates the effects of OMT). OMT, oxymatrine; PIP2, phosphorylating phosphatidylinositol-4,5-bisphosphate; PIP3, phosphatidylinositol-3,4,5-trisphosphate, p, phosphorylated.

caspase-9, glycogen synthase kinase-3- and p21, facilitating cell proliferation triggered by insulin and growth factors and encouraging cell survival. Hence, AKT is a key anti-apoptotic regulator (62). The PI3K/AKT pathway has been reported to be abnormally active in PF (63). OMT regulates the PI3K/AKT pathway in hypoxic-ischemic brain damage and colitis (31,38). It was hypothesized that PI3K/AKT signaling is implicated in pathogenesis of PF and that OMT protects against PF partially via the PI3K/AKT pathway. In the present study, OMT exhibited the potential to reverse PF by activating the PI3K/AKT pathway (Fig. 6). However, a previous review suggested that PI3K/AKT inhibitors are beneficial in PF treatment (1). Baicalin alleviates PF by decreasing p-AKT levels in lung fibroblasts (22). Ligustrazine attenuates paraquat-induced PF by blocking PI3K/AKT/mTOR signaling in mouse lung tissue (64). The differences in the findings of these studies could be attributed to the different research subjects. PF is characterized by excessive apoptosis of fine bronchial and AECs, destroying alveolar structural integrity and inhibiting pulmonary fibroblast apoptosis (13,65). During fibrosis, AECs undergo injury, apoptosis, fibroblast proliferation, and fibroblast to myofibroblast conversion; at this point, the main cells present in the fibrotic tissue of the lung are fibroblasts and myofibroblasts. Thus, inhibition of PI3K/AKT signaling, which promotes fibroblast and myofibroblast apoptosis, abrogates fibroblast proliferation and collagen production in response to bleomycin (66). In the present study, OMT upregulated PI3K/AKT signaling and inhibited AEC apoptosis, thus inhibiting PF.

The present study had some limitations. The present study primarily investigated the inhibition of the PI3K/AKT pathway. Further research on PI3K/AKT pathway activators is needed to corroborate the present findings. Additionally, the PI3K/AKT signaling pathway involves multiple cytokines and these downstream cytokines may be regulated by factors other than PI3K. Thus, more research on the effects of these downstream cytokines on the antifibrotic activity of OMT is required. Furthermore, only *in vitro* cell-based experiments were performed and further *in vivo* research using animal models is needed to validate the anti-PF properties of OMT. The lack of OMT-alone treatment group for comparison was also a limitation of the present study.

In summary, the present study showed that OMT attenuates TGF-β1-mediated mitochondrial apoptosis signaling in AECs by activating the PI3K/AKT signaling pathway. Based on these findings, OMT may be a potential therapeutic agent for PF.

Acknowledgements

Not applicable.

Funding

The present study was supported by the Key Laboratory of Geriatrics Respiratory Disease Education Department of Sichuan [grant no. (2015) 603] and Research Fund of Chengdu Medical College (grant no: CYFY2017GLPXH08 CYFY2018GLPXH01).

Availability of data and materials

The datasets used and/or analyzed during the current study are available from the corresponding author on reasonable request.

Authors' contributions

TF designed the study. PZ, QL and JQ performed experiments. RD and WL analyzed the data. TF and RD wrote the manuscript. TF and RD confirm the authenticity of all the raw data. All authors have read and approved the final manuscript.

Ethics approval and consent to participate

Not applicable.

Patient consent for publication

Not applicable.

Competing interests

The authors declare that they have no competing interests.

References

1. Wang J, Hu K, Cai X, Yang B, He Q, Wang J and Weng Q: Targeting PI3K/AKT signaling for treatment of idiopathic pulmonary fibrosis. Acta Pharm Sin B 12: 18-32, 2022.
2. Yanagihara T, Sato S, Upagupta C and Kolb M: What have we learned from basic science studies on idiopathic pulmonary fibrosis? Eur Respir Rev 28: 190029, 2019.
3. Otoupalova E, Smith S, Cheng G and Thannickal VJ: Oxidative stress in pulmonary fibrosis. Compr Physiol 10: 509-547, 2020.
4. Richeldi L, Collard HR and Jones MG: Idiopathic pulmonary fibrosis. Lancet 389: 1941-1952, 2017.
5. Somogyi V, Chaudhuri N, Torrisi SE, Kahn N, Müller V and Kreuter M: The therapy of idiopathic pulmonary fibrosis: What is next? Eur Respir Rev 28: 190021, 2019.
6. Kropski JA and Blackwell TS: Progress in understanding and treating idiopathic pulmonary fibrosis. Annu Rev Med 70: 211-224, 2019.
7. Tepede A and Yogaratnam D: Nintedanib for idiopathic pulmonary fibrosis. J Pharm Pract 32: 199-206, 2019.
8. George PM, Patterson CM, Reed AK and Thillai M: Lung transplantation for idiopathic pulmonary fibrosis. Lancet Respir Med 7: 271-282, 2019.

9. Chambers DC, Cherikh WS, Harhay MO, Hayes D Jr, Hsich E, Khush KK, Meiser B, Potena L, Rossano JW, Toll AE, *et al*: The international thoracic organ transplant registry of the international society for heart and lung transplantation: Thirty-sixth adult lung and heart-lung transplantation Report-2019; Focus theme: Donor and recipient size match. J Heart Lung Transplant 38: 1042-1055, 2019.
10. Fattman CL: Apoptosis in pulmonary fibrosis: Too much or not enough? Antioxid Redox Signal 10: 379-385, 2008.
11. Olajuyin AM, Zhang X and Ji HL: Alveolar type 2 progenitor cells for lung injury repair. Cell Death Discov 5: 63, 2019.
12. Corrin B, Dewar A, Rodriguez-Roisin R and Turner-Warwick M: Fine structural changes in cryptogenic fibrosing alveolitis and asbestosis. J Pathol 147: 107-119, 1985.
13. Myers JL and Katzenstein AL: Epithelial necrosis and alveolar collapse in the pathogenesis of usual interstitial pneumonia. Chest 94: 1309-1311, 1988.
14. Li XP, Shu RJ, Filippatos G and Uhal BD: Apoptosis in lung injury and remodeling. J Appl Physiol (1985) 97: 1535-1542, 2004.
15. Uhal BD, Joshi I, Hughes WF, Ramos C, Pardo A and Selman M: Alveolar epithelial cell death adjacent to underlying myofibroblasts in advanced fibrotic human lung. Am J Physiol 275: L1192-L1199, 1998.
16. Barbas-Filho JV, Ferreira MA, Sesso A, Kairalla RA, Carvalho CR and Capelozzi VL: Evidence of type II pneumocyte apoptosis in the pathogenesis of idiopathic pulmonary fibrosis (IFP)/usual interstitial pneumonia (UIP). J Clin Pathol 54: 132-138, 2001.
17. Chen F, Gong L, Zhang L, Wang H, Qi X, Wu X, Xiao Y, Cai Y, Liu L, Li X and Ren J: Short courses of low dose dexamethasone delay bleomycin-induced lung fibrosis in rats. Eur J Pharmacol 536: 287-295, 2006.
18. Bock FJ and Tait SWG: Mitochondria as multifaceted regulators of cell death. Nat Rev Mol Cell Biol 21: 85-100, 2020.
19. Budinger GR, Mutlu GM, Eisenbart J, Fuller AC, Bellmeyer AA, Baker CM, Wilson M, Ridge K, Barrett TA, Lee VY and Chandel NS: Proapoptotic Bid is required for pulmonary fibrosis. Proc Natl Acad Sci USA 103: 4604-4609, 2006.
20. Hu X, Xu Q, Wan H, Hu Y, Xing S, Yang H, Gao Y and He Z: PI3K-AKT-mTOR/PFKFB3 pathway mediated lung fibroblast aerobic glycolysis and collagen synthesis in lipopolysaccharide-induced pulmonary fibrosis. Lab Invest 100: 801-811, 2020.
21. Engelman JA, Luo J and Cantley LC: The evolution of phosphatidylinositol 3-kinases as regulators of growth and metabolism. Nat Rev Genet 7: 606-619, 2006.
22. Zhao H, Li C, Li L, Liu J, Gao Y, Mu K, Chen D, Lu A, Ren Y and Li Z: Baicalin alleviates bleomycin-induced pulmonary fibrosis and fibroblast proliferation in rats via the PI3K/AKT signaling pathway. Mol Med Rep 21: 2321-2334, 2020.
23. Schmitt-Ney M: The FOXO's advantages of being a family: Considerations on function and evolution. Cells 9: 787, 2020.
24. Li H, Kan B, Song L, Liu Y and Jian X: Role of the Hippo signaling pathway in safflower yellow pigment treatment of paraquat-induced pulmonary fibrosis. J Int Med Res 48: 300060520905425, 2020.
25. Takano M, Deguchi J, Senoo S, Izumi M, Kawami M and Yumoto R: Suppressive effect of quercetin against bleomycin-induced epithelial-mesenchymal transition in alveolar epithelial cells. Drug Metab Pharmacokinet 35: 522-526, 2020.
26. Sun X, Cui X, Chen X and Jiang X: Baicalein alleviated TGF β1-induced type I collagen production in lung fibroblasts via downregulation of connective tissue growth factor. Biomed Pharmacother 131: 110744, 2020.
27. Zhou Y, Zhu WP, Cai XJ and Chen M: Atomized paclitaxel liposome inhalation treatment of bleomycin-induced pulmonary fibrosis in rats. Genet Mol Res 15: 10, 2016.
28. Hu Y, Li M, Zhang M and Jin Y: Inhalation treatment of idiopathic pulmonary fibrosis with curcumin large porous microparticles. Int J Pharm 551: 212-222, 2018.
29. Zhang YY, Yi M and Huang YP: Oxymatrine ameliorates doxorubicin-induced cardiotoxicity in rats. Cell Physiol Biochem 43: 626-635, 2017.
30. Xiang X, Tu C, Li Q, Wang W, Huang X, Zhao Z, Xiong H and Mei Z: Oxymatrine ameliorates imiquimod-induced psoriasis pruritus and inflammation through inhibiting heat shock protein 90 and heat shock protein 60 expression in keratinocytes. Toxicol Appl Pharmacol 405: 115209, 2020.
31. Wang D, Lou XQ, Jiang XM, Yang C, Liu XL and Zhang N: Oxymatrine protects against the effects of cardiopulmonary resuscitation via modulation of the TGF-β1/Smad3 signaling pathway. Mol Med Rep 17: 4747-4752, 2018.
32. Ying XJ, Jin B, Chen XW, Xie J, Xu HM and Dong P: Oxymatrine downregulates HPV16E7 expression and inhibits cell proliferation in laryngeal squamous cell carcinoma Hep-2 cells in vitro. Biomed Res Int 2015: 150390, 2015.
33. Liu Y, Xu Y, Ji W, Li X, Sun B, Gao Q and Su C: Anti-tumor activities of matrine and oxymatrine: Literature review. Tumour Biol 35: 5111-5119, 2014.
34. Song WJ, Luo J, Wu T and Yao SK: Oral oxymatrine preparation for chronic hepatitis B: A systematic review of randomized controlled trials. Chin J Integr Med 22: 141-149, 2016.
35. Shi HJ, Zhou H, Ma AL, Wang L, Gao Q, Zhang N, Song HB, Bo KP and Ma W: Oxymatrine therapy inhibited epidermal cell proliferation and apoptosis in severe plaque psoriasis. Br J Dermatol 181: 1028-1037, 2019.
36. Huang Y, Li X, Zhang X and Tang J: Oxymatrine ameliorates memory impairment in diabetic rats by regulating oxidative stress and apoptosis: Involvement of NOX2/NOX4. Oxid Med Cell Longev 2020: 3912173, 2020.
37. Chen Q, Duan X, Fan H, Xu M, Tang Q, Zhang L, Shou Z, Liu X, Zuo D, Yang J, *et al*: Oxymatrine protects against DSS-induced colitis via inhibiting the PI3K/AKT signaling pathway. Int Immunopharmacol 53: 149-157, 2017.
38. Liu Y, Wang H, Liu N, Du J, Lan X, Qi X, Zhuang C, Sun T, Li Y and Yu J: Oxymatrine protects neonatal rat against hypoxic-ischemic brain damage via PI3K/AKT/GSK3β pathway. Life Sci 254: 116444, 2020.
39. Liu L, Lu W, Ma Z and Li Z: Oxymatrine attenuates bleomycin-induced pulmonary fibrosis in mice via the inhibition of inducible nitric oxide synthase expression and the TGF-β/Smad signaling pathway. Int J Mol Med 29: 815-822, 2012.
40. Morikawa M, Derynck R and Miyazono K: TGF-β and the TGF-β family: Context-dependent roles in cell and tissue physiology. Cold Spring Harb Perspect Biol 8: a021873, 2018.
41. Kim KK, Sheppard D and Chapman HA: TGF-β1 signaling and tissue fibrosis. Cold Spring Harb Perspect Biol 10: 34, 2018.
42. Zhang C, Zhu X, Hua Y, Zhao Q, Wang K, Zhen L, Wang G, Lü J, Luo A, Cho WC, *et al*: YY1 mediates TGF-β1-induced EMT and pro-fibrogenesis in alveolar epithelial cells. Respir Res 20: 249, 2019.
43. Chen X, Sun R, Hu J, Mo Z, Yang Z, Liao D and Zhong N: Attenuation of bleomycin-induced lung fibrosis by OMT is associated with regulation of fibroblast proliferation and collagen production in primary culture. Basic Clin Pharmacol Toxicol 103: 278-286, 2008.
44. Livak KJ and Schmittgen TD: Analysis of relative gene expression data using real-time quantitative PCR and the 2(-Delta Delta C(T)) method. Methods 25: 402-408, 2001.
45. Ruwanpura SM, Thomas BJ and Bardin PG: Pirfenidone: Molecular mechanisms and potential clinical applications in lung disease. Am J Respir Cell Mol Biol 62: 413-422, 2020.
46. Hosseini SA, Zahedipour F, Sathyapalan T, Jamialahmadi T and Sahebkar A: Pulmonary fibrosis: Therapeutic and mechanistic insights into the role of phytochemicals. Biofactors 47: 250-269, 2021.
47. Hu C, Wang Y, Fan Y, Li H, Wang C, Zhang J, Zhang S, Han X and Wen C: Lipidomics revealed idiopathic pulmonary fibrosis-induced hepatic lipid disorders corrected with treatment of baicalin in a murine model. AAPS J 17: 711-722, 2015.
48. Elmore S: Apoptosis: A review of programmed cell death. Toxicol Pathol 35: 495-516, 2007.
49. Kumar RK: Idiopathic pulmonary fibrosis: An epithelial/fibroblasticcross-talk disorder. Respir Res 3: 29, 2002.
50. Snijder J, Peraza J, Padilla M, Capaccione K and Salvatore MM: Pulmonary fibrosis: A disease of alveolar collapse and collagen deposition. Expert Rev Respir Med 13: 615-619, 2019.
51. Guillot L, Nathan N, Tabary O, Thouvenin G, Rouzic PL, Corvol H, Amselem S and Clement A: Alveolar epithelial cells: Master regulators of lung homeostasis. Int J Biochem Cell Biol 45: 2568-2573, 2013.
52. Serrano-Mollar A: Alveolar epithelial cell injury as an etiopathogenic factor in pulmonary fibrosis. Arch Bronconeumol 48: 2-6, 2012 (In Spanish).
53. Lu J, Wu L, Wang X, Zhu J, Du J and Shen B: Detection of mitochondria membrane potential to study CLIC4 knockdown-induced HN4 cell apoptosis in vitro. J Vis Exp 137: 56137, 2018.
54. Hill C, Jones MG, Davies DE and Wang Y: Epithelial-mesenchymal transition contributes to pulmonary fibrosis via aberrant epithelial/fibroblastic cross-talk. J Lung Health Dis 3: 31-35, 2019.

55. Wang YC, Liu JS, Tang HK, Nie J, Zhu JX, Wen LL and Guo QL: miR 221 targets HMGA2 to inhibit bleomycin induced pulmonary fibrosis by regulating TGF β1/Smad3-induced EMT. Int J Mol Med 38: 1208-1216, 2016.
56. Liu Y, Li Y, Xu Q, Yao W, Wu Q, Yuan J, Yan W, Xu T, Ji X and Ni C: Long non-coding RNA-ATB promotes EMT during silica-induced pulmonary fibrosis by competitively binding miR-200c. Biochim Biophys Acta Mol Basis Dis 1864: 420-431, 2018.
57. Braun F, de Carné Trécesson S, Bertin-Ciftci J and Juin P: Protect and serve: Bcl-2 proteins as guardians and rulers of cancer cell survival. Cell Cycle 12: 2937-2947, 2013.
58. Willis S, Day CL, Hinds MG and Huang DC: The Bcl-2-regulated apoptotic pathway. J Cell Sci 15: 4053-4056, 2003.
59. Kuwano K, Hagimoto N, Tanaka T, Kawasaki M, Kunitake R, Miyazaki H, Kaneko Y, Matsuba T, Maeyama T and Hara N: Expression of apoptosis-regulatory genes in epithelial cells in pulmonary fibrosis in mice. J Pathol 190: 221-229, 2000.
60. Youle RJ and Strasser A: The BCL-2 protein family: Opposing activities that mediate cell death. Nat Rev Mol Cell Biol 9: 47-59, 2008.
61. Franke TF, Hornik CP, Segev L, Shostak GA and Sugimoto C: PI3K/AKT and apoptosis: Size matters. Oncogene 22: 8983-8998, 2003.
62. Liu R, Chen Y, Liu G, Li C, Song Y, Cao Z, Li W, Hu J, Lu C and Liu Y: PI3K/AKT pathway as a key link modulates the multidrug resistance of cancers. Cell Death Dis 11: 797, 2020.
63. Sun Y, Zhang Y and Chi P: Pirfenidone suppresses TGF-β1-induced human intestinal fibroblasts activities by regulating proliferation and apoptosis via the inhibition of the Smad and PI3K/AKT signaling pathway. Mol Med Rep 18: 3907-3913, 2018.
64. Liu MW, Su MX, Tang DY, Hao L, Xun XH and Huang YQ: Ligustrazin increases lung cell autophagy and ameliorates paraquat-induced pulmonary fibrosis by inhibiting PI3K/AKT/mTOR and hedgehog signalling via increasing miR-193a expression. BMC Pulm Med 19: 35, 2019.
65. Moodley YP, Caterina P, Scaffidi AK, Misso NL, Papadimitriou JM, McAnulty RJ, Laurent GJ, Thompson PJ and Knight DA: Comparison of the morphological and biochemical changes in normal human lung fibroblasts and fibroblasts derived from lungs of patients with idiopathic pulmonary fibrosis during FasL-induced apoptosis. J Pathol 202: 486-495, 2004.
66. Lu Y, Azad N, Wang L, Iyer AK, Castranova V, Jiang BH and Rojanasakul Y: Phosphatidylinositol-3-kinase/AKT regulates bleomycin-induced fibroblast proliferation and collagen production. Am J Respir Cell Mol Biol 42: 432-441, 2010.